Restricted Conformational Flexibility of a Triphenylamine Derivative on the Formation of Host–Guest Complexes with Various Macrocyclic Hosts

ARTICLE *in* CHEMISTRY - A EUROPEAN JOURNAL · MARCH 2012

Impact Factor: 5.73 · DOI: 10.1002/chem.201103079 · Source: PubMed

4 AUTHORS, INCLUDING:

Amal kumar Mandal
University of Twente
34 PUBLICATIONS **494** CITATIONS
SEE PROFILE

Priyadip Das
Central Salt and Marine Chemicals Researc…
27 PUBLICATIONS **328** CITATIONS
SEE PROFILE

Amitava Das
CSIR - National Chemical Laboratory, Pune
195 PUBLICATIONS **4,696** CITATIONS
SEE PROFILE

CHEMISTRY
A EUROPEAN JOURNAL

DOI: 10.1002/chem.201103079

Restricted Conformational Flexibility of a Triphenylamine Derivative on the Formation of Host–Guest Complexes with Various Macrocyclic Hosts

Amal Kumar Mandal, Moorthy Suresh, Priyadip Das, and Amitava Das*[a]

Abstract: Herein, we report the host–guest-type complex formation between the host molecules cucurbit[7]uril (CB[7]), β-cyclodextrin (β-CD), and dibenzo[24]crown-8 ether (DB24C8) and a newly synthesized triphenylamine (TPA) derivative $\mathbf{1X}_3$ as the guest component. The host–guest complex formation was studied in detail by using ^{1}H NMR, 2D NOESY, UV/Vis fluorescence, and time-resolved emission spectroscopy. The chloride salt of the TPA derivative was used for recognition studies with CB[7] and β-CD in an aqueous medium. The restricted internal rotation of the guest molecule on complex formation with either of these two host molecules was reflected in the enhancement of the emission quantum yield and the average excited-state lifetime for the triphenylamine-based excited states. Studies with DB24C8 as the host molecule were performed in dichloromethane, a medium that maximizes the noncovalent interaction between the host and guest fragments. The Förster resonance energy transfer (FRET) process involving DB24C8 and $\mathbf{1}(PF_6)_3$, as the donor and acceptor fragments, respectively, was established by electrochemical, steady-state emission, and time-correlated single-photon counting studies.

Keywords: host–guest systems · internal rotation · noncovalent interactions · pseudorotaxanes · resonance energy transfer

Introduction

Achieving designer, interwoven complexes, such as pseudorotaxanes, rotaxanes, and catenanes, with appropriately substituted host and guest fragments to realize an assembly that shows a special property is of current research interest.[1] Various nonbonding interactions such as π–π,[2] hydrogen-bonding,[3] hydrophobic, and van der Waals interactions are generally operational for the generation and stabilization of these supramolecular architectures.[4] Chemists have achieved predictable control over these noncovalent interactions and have used these weak forces in their favor to develop a plethora of intricate functional structures. In most examples, a combination of various nonbonding interactions is operational to stabilize such intricate supramolecular architectures. A change of any or a combination of these interactions may allow host molecules to adopt different relative conformations/orientations in the host–guest assembly. This outcome opens up the possibility of achieving desired intercomponent molecular movements as a result of the inclusion-complex formation under the influence of an appropriate external stimulation. Such host or guest molecules, appropriately substituted with a chromogenic fragment, offer the possibility of probing such conformational or structural changes on inclusion-complex formation by monitoring associated electronic or fluorescence spectral changes. However, reports on probing such a change in molecular conformation or relative orientation due to inclusion-complex formation by monitoring changes in the electronic or luminescence properties are not very common.[5]

It has been reported that triphenylamine (TPA) and several of its derivatives have drawn much attention from researchers with varying interests due to their huge application potential in diverse areas, such as, organic light-emitting diodes (OLED),[6] photoconductors,[7] laser dyes, and mechanoluminescent materials.[8] Previous reports of structural[9] and theoretical studies[10] on TPA suggest that this molecule preferentially adopts a three-bladed propeller structure with a planar or nearly planar central N-C-C-C moiety. A symmetric top geometry for TPA with at least C_3 symmetry is proposed in the gas phase. Each of the three phenyl groups in TPA is symmetrically twisted from the plane and makes the propeller blade. Due to the deviation of the three phenyl ring from coplanarity, TPA and its derivatives adopt a 3D structure. Two different opposing forces, namely, the energy-lowering π-conjugation of the phenyl ring and steric repulsion between the inner-ring hydrogen atoms, are generally operational and control this conformation in different TPA derivatives. The steric repulsion between the inner-ring hydrogen atoms is highest for the perfectly planar conformation, which actually makes TPA a conformationally flexible molecule. This conformational flexibility of TPA derivatives has a direct relevance to their photoluminescence property because a fast nonradiative relaxation of the excited state of these compounds is favored. The lack of rigidity in the twist-

[a] A. K. Mandal, M. Suresh, P. Das, Dr. A. Das
Central Salt and Marine Chemicals Research Institute (CSIR)
Bhavnagar, 364002 Gujarat (India)
Fax: (+91) 278-2567562
E-mail: amitava@csmcri.org

Supporting information for this article is available on the WWW under http://dx.doi.org/10.1002/chem.201103079.

ed TPA derivatives also adversely affects their application potential as a host material in OLEDs.[11]

All these approaches have initiated a surge of interest among researchers to understand how the flexibility of these molecules can be controlled to achieve the desired photophysical properties. However, efforts in this regard are mostly restricted to the synthesis of highly rigid framework TPA derivatives.[12] It is known that macrocyclic hosts impose a structural confinement on the included chromophoric guest molecules and suppress the nonradiative relaxation processes associated with the various molecular movements/vibrations, which in turn improves the luminescence quantum yield and the lifetime of the photoexcited states.[13] Among various macrocyclic hosts, cyclodextrin (CD) and cucurbit[*n*]uril (CB[*n*]) are most commonly used for such studies. However, to the best of our knowledge no such report with a TPA derivative as a guest molecule has been reported to unveil the influence of inclusion-complex formation on the luminescence properties.

Cucurbiturils (CB[*n*]; $n=5$–8, 10) are composed of *n* glycoluril units that are coupled in a cyclic manner by 2*n* methylene bridges. The pumpkin-shaped CB[*n*] molecules are highly symmetrical cage structures with two identical portal ends flanked with highly polarizable ureido carbonyl groups and an interior hydrophobic cavity. The presence of the internal hydrophobic cavity, accessible by two carbonyl openings induces ion–dipole, dipole–dipole, and hydrogen-bonding interactions, thus making this molecule favorable for inclusion-complex formation with various guest molecules.[14] The CB[*n*] molecules have a common depth (9.1 Å), but their equatorial widths (5.4 Å for $n=7$), annular widths (7.3 Å for $n=7$), and volumes vary systematically with ring size. The portals that guard the entry to CB[7] are narrower than the cavity itself by approximately 2 Å, which results in constrictive binding that induces significant steric barriers to guest association and dissociation.

β-Cyclodextrin (β-CD) is another commonly used host molecule, built up from seven glucopyranose subunits that are connected at the 1,4-position. As a consequence of the $^4C_1$ conformation of the glucopyranose units, all the secondary hydroxy groups are situated on one of the two edges of the ring, whereas all the primary hydroxy groups are placed on the other edge. This makes the β-CD ring adopt a conical cylinder structure. The electrostatic potential at the portals and within the cavity of CB[7] is significantly more negative than β-CD. This difference in electrostatic potential has significance in their recognition behavior and the relative stability of the respective host–guest complexes.

A wide range of guests have been shown to form stable inclusion complexes with cucurbiturils, including cations,[15,21] neutral species,[16] and anions,[17] thus indicating the versatility and potential usefulness of a cucurbituril as a host molecule. Whereas CDs can be used to accommodate a variety of small organic molecules.[18] Apart from these two host molecules, various crown ether derivatives are another type of synthetic host for a wide variety of cationic guests. Various guests, such as, metal ions, primary alkyl ammonium ions (RNH_3^+),[19c,d] secondary dialkyl ammonium ions ($R_2NH_2^+$),[19] and imidazolium cations,[20] have received considerable attention among the many guest species that have been investigated.

We used the three different host molecules CB[7], β-CD, and DB24C8 to study inclusion-complex formation with a secondary ammonium salt of a TPA derivative (Figure 1). These host molecules have comparable cavity volume, but differ in geometrical features, solubilities, and association patterns with the ammonium salt-based guest molecules. Restricted tortional motion of the secondary ammonium salt of

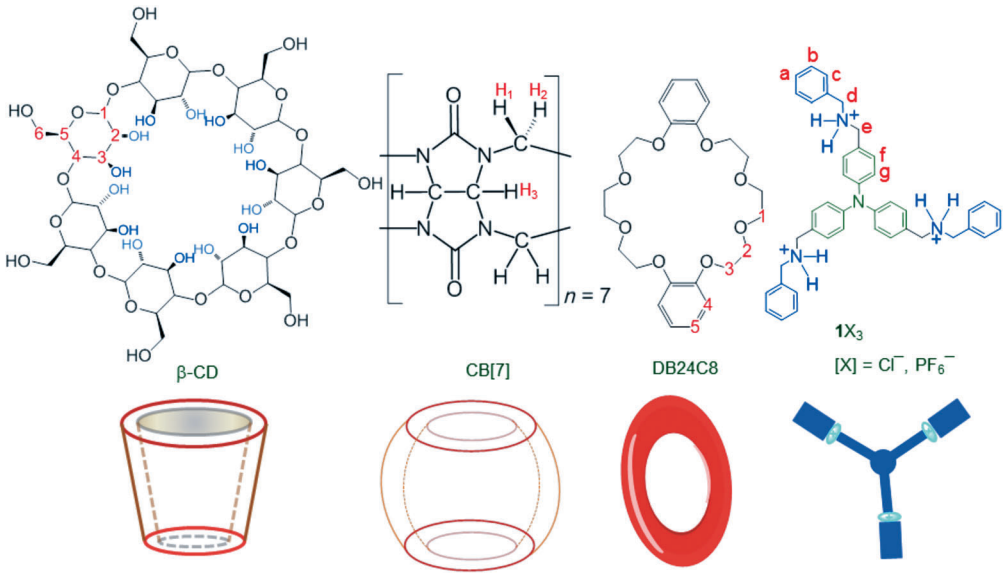

Figure 1. Schematic representation of the different macrocyclic hosts and guest molecules used in this study.

the TPA derivative on inclusion-complex formation with different macrocylic host molecules is expected to improve the emission quantum yield of the TPA core by suppressing the nonradiative deactivation of the excited states. This behavior offers an opportunity to probe the formation of such an inclusion complex by monitoring the emission response of the TPA-based fragment. More importantly, studies with three different host molecules and a common guest molecule allow a direct comparison of the structural aspects of the host molecules in influencing the relative stability of the different host–guest complexes thus formed. For each host–guest complex formation, the respective binding stoichiometries and association constants, along with the relative geometries of the host–guest complexes were studied by using 1D and 2D ^{1}H NMR spectroscopy, mass spectrometry (MS), steady-state fluorescence spectroscopy, and time-resolved studies using time-correlated single-photon counting (TCSPC) technique.

Results and Discussion

The secondary ammonium salt of TPA derivatives (**1**X_3; X = Cl^- or PF_6^-) were synthesized by treating benzylamine with tris(*para*-formylphenyl)amine, and the obtained intermediate was further reduced with $NaBH_4$ in methanol. The respective amine was protonated with the appropriate acid and isolated as a chloride salt, which was soluble in water and used for recognition studies with CB[7] and β-CD because these hosts are only soluble in water. Complexation studies with DB24C8 were performed in CH_2Cl_2; therefore, the hexafluorophosphate salt of the protonated TPA derivative was used.

Complexation of 1Cl$_3$ with CB[7]: The binding interaction between **1**Cl_3 and CB[7] was monitored by ^{1}H NMR spectroscopic analysis. Structurally, CB[7] has two distinctly different binding regions: 1) the hydrophobic cavity and 2) the outer disk formed by the oxygen atoms that stabilize the positive charge or cations. The guest protons located within the hydrophobic cavity are expected to be shielded for the ^{1}H NMR spectral signal ($\Delta\delta < 0$), whereas guest protons located at the more polar outer C=O cavity are deshielded ($\Delta\delta > 0$).

Figure 2 shows the ^{1}H NMR spectra of **1**Cl_3 recorded in D_2O in the absence (Figure 2a) and presence of CB[7] (Figure 2b–d) and reveals that the chemical shift of all the protons of **1**Cl_3 are shifted on host–guest inclusion-complex formation relative to free **1**Cl_3. A closer look at the Figure 2 reveals that the signals for two sets of aliphatic protons of **1**Cl_3 shift in opposite directions; that is, an upfield shift of approximately $\Delta\delta = 0.4$ ppm is observed for H_d, whereas a downfield shift of approximately $\Delta\delta = 0.19$ ppm is evident for H_e. These chemical shifts indicate that H_d of **1**Cl_3 is included inside the shielding region of the CB[7] cavity and H_e of **1**Cl_3 is located in the deshielding region, outside of the carbonyl portal. Appreciable shifts are also observed for

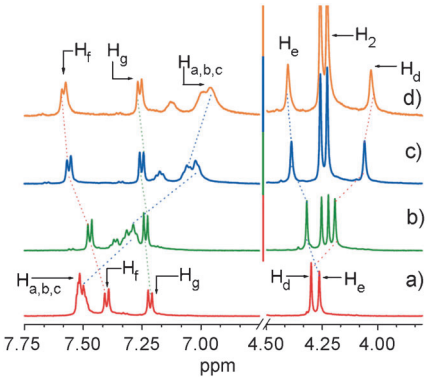

Figure 2. Partial ^{1}H NMR spectra (500 MHz, D_2O, 298 K) of **1**Cl_3 (3.7×10^{-3} M) with increasing [CB[7]]. a) In the absence of CB[7] and in the presence of b) 1.0, c) 2.0, and d) 3.0 equivalents of CB[7].

the aromatic protons of **1**Cl_3 on formation of an inclusion complex with CB[7] (Figure 2). The ^{1}H NMR signals that correspond to the aromatic protons of the benzyl unit (H_a, H_b, and H_c) are broadened with an upfield shift of approximately $\Delta\delta = 0.83$ ppm, whereas the signals for the other aromatic protons H_g and H_f of **1**Cl_3 are shifted downfield ($\Delta\delta \approx 0.06$ and 0.28 ppm for H_g and H_f, respectively). The downfield shifts of signals for the H_g and H_f protons and the significant upfield shifts of the signals for the benzyl H_a, H_b, and H_c protons on inclusion-complex formation are consistent with the fact that CB[7] engulfs the benzyl unit inside its cavity, whereas the H_g and H_f protons interact with the carbonyl oxygen atoms of the host portal. These outcomes suggest the formation of an "external" inclusion complex with **1**Cl_3. Presumably, steric hindrance could play a key role in determining the main binding site for CB[7] and allow the inclusion of a benzyl unit rather than the phenyl moiety of the TPA core. Such an "external" complex formation was has been reported previously for the inclusion complex formed between CB[7] and different derivatives of viologen as guest species.[21]

To gain insight into the molecular interaction and the geometry of the host–guest complex, we performed 2D ^{1}H NMR spectroscopic studies. The NOESY spectrum of **1**Cl_3 in presence of three molar equivalents of CB[7] were recorded (Figure 3a) and shows cross-peaks between the protons (H_1, H_2, H_3) of CB[7] and the aromatic protons of **1**Cl_3. These cross-peaks corroborate the formation of an inclusion complex between CB[7] and **1**Cl_3 in aqueous solution, whereas the binding interactions seem to be dominated by hydrophobic forces, with one of the two aromatic rings being included in the CB[7] cavity. It is anticipated that the host–guest complex would experience increased steric crowding when CB[7] engulfs the phenyl ring of the TPA core rather than the external benzyl moiety of **1**Cl_3 inside its cavity. Thus, the experimental data tend to imply that CB[7] preferred the formation of an "external" inclusion complex.

The changes in the chemical shift values ($\Delta\delta$ in ppm) for H_e of **1**Cl_3 in the ^{1}H NMR spectrum with varying concentrations of CB[7] in D_2O were used for a Job plot analysis (Fig-

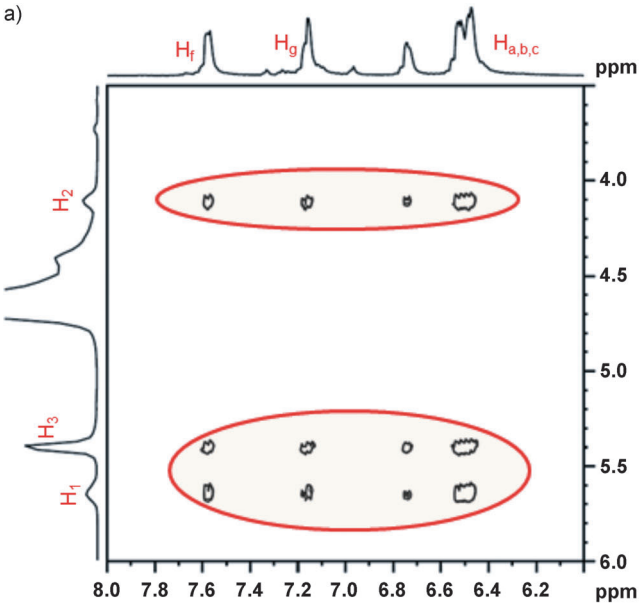

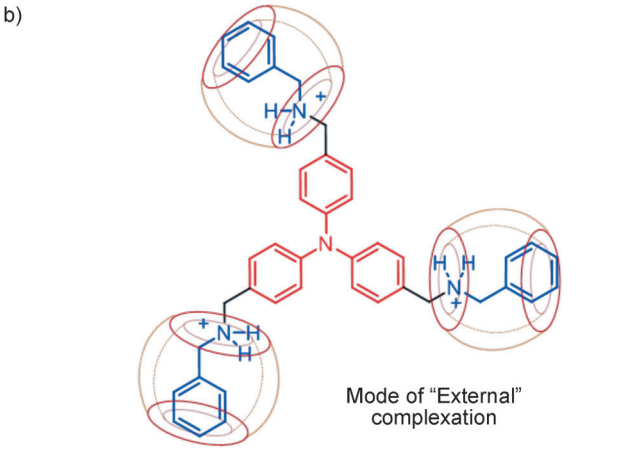

Figure 3. a) Partial 2D NOESY NMR spectrum (500 MHz, D_2O, 298 K) of a solution of $\mathbf{1}Cl_3$ (3.7×10^{-3} M) and CB[7] (11.2×10^{-3} M). b) Mode of binding interaction between $\mathbf{1}Cl_3$ and CB[7] is shown.

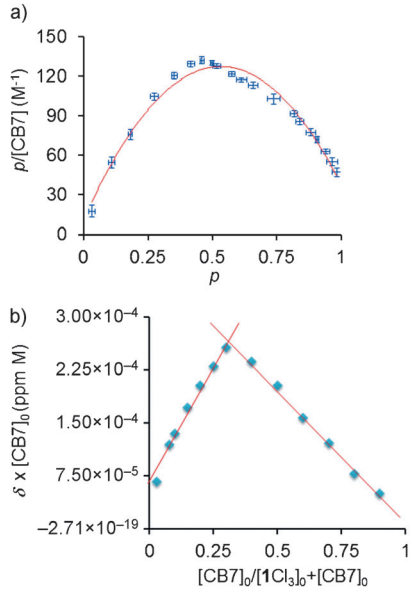

Figure 4. a) Scatchard plot for the complexation of $\mathbf{1}Cl_3$ with CB[7] (D_2O, 25 °C, $[\mathbf{1}Cl_3]_0=3.7\times10^{-3}$ M; $y=-407.59x^2+433.88x+11.824$, $r^2=0.98$), where p is the fraction of $\mathbf{1}Cl_3$ units bound. Error bars in $p=\pm0.02$; error bar in $p/[CB7]=\pm0.87$. b) Job plot that reveals a 1:3 binding stoichiometry between $\mathbf{1}Cl_3$ and CB[7] in D_2O by using changes in the chemical shift δ data for H_e ($[\mathbf{1}Cl_3]_0+[CB7]_0=6.8\times10^{-3}$ M).

ure 4b), which signified a 1:3 binding stoichiometry for the inclusion-complex formation between $\mathbf{1}Cl_3$ and CB[7]. A Scatchard plot (Figure 4a) was drawn to study the relationship between the three binding sites of $\mathbf{1}Cl_3$ during complex formation with CB[7]. The nonlinear nature of this plot with a maximum value reveals that positive cooperativity drives the complex-formation process.[22]

Analysis of the Scatchard plot enabled us to find out the stoichiometric binding constants K_1, K_2, and K_3 and the apparent average association constant K_{av}. From the plot of $p/[CB7]$ versus p (p = extent of complexation; Figure 4a), the intercept on the $p/[CB7]$ axis gave the value of $K_1=(1.2\pm0.5)\times10^1\,M^{-1}$. The initial slope of the first six data points for low values of p (Figure 4a) gave the value of $2K_2-K_1$ to give $K_2=(1.5\pm2.6)\times10^2\,M^{-1}$. The final slope, calculated from last nine data points for high values of p, gave the value of $-3K_3$[22b] to give $K_3=(1.0\pm1.9)\times10^2\,M^{-1}$ and $K_{av}=(K_1+K_2+K_3)/3=(9.0\pm1.2)\times10^1\,M^{-1}$ (see the Supporting Information for further details).[22d] On the basis of on the above information, a structural representation of the inclusion complex $\mathbf{1}Cl_3\cdot3$CB[7] is shown in Figure 3b.

ESI mass-spectrometric studies were performed to confirm the host–guest complex formation and establish the binding stoichiometry. The mass spectrum was dominated by signals that correspond to the inclusion complexes with a 1:3 binding stoichiometry (Table 1). The calculated and observed masses for $\mathbf{1}Cl_3\cdot3$CB[7] are summarized in Table 1.

Table 1. The MALDI-TOF and ESI mass spectrometric data for the inclusion complex $\mathbf{1}Cl_3\cdot3$G (G = CB[7], β-CD, or DB24C8).

Host–guest system	Molecular formula	m/z calcd	m/z observed
$\mathbf{1}Cl_3\cdot3$CB[7]	$\{\mathbf{1}Cl_3+3CB[7]+H_2O-3Cl\}^{3+}/3$	1369.59	1369.02, 1369.32, 1369.65[a]
$\mathbf{1}Cl_3\cdot3$β-CD	$\{\mathbf{1}Cl_3+3β\text{-}CD-3Cl+H_2O\}^{3+}/3$	1342.16	1341.45, 1341.75, 1342.13[a]
$\mathbf{1}(PF_6)_3\cdot3$DB24C8	$\{\mathbf{1}(PF_6)_3+3DB+Na\}^{+}$	2409.52	2409.55[b]
	$\{\mathbf{1}(PF_6)_3+3DB-3PF_6\}^{3+}/3$	650.52	650.16, 650.48, 650.81[c]

[a] ESI mass spectrometric data were recorded in the positive-ion mode with water as the solvent. [b] MALDI-TOF mass spectrometric data were recorded in the positive-ion mode with CH_2Cl_2/CH_3CN (4:1, v/v) as the solvent. [c] ESI mass spectroscopic data were recorded in the positive-ion mode with CH_2Cl_2/CH_3CN (4:1, v/v) as the solvent.

Complexation of $1Cl_3$ with β-CD: Four protons H_1, H_2, H_4, and H_6 are located on the external surface of the molecule in β-CD, whereas other two protons H_3 and H_5 are in the interior of the cavity at the wide and narrow rims, respectively. Thus, the signals for H_3 and H_5 are expected to be mostly influenced on inclusion-complex formation and are most sensitive to the inclusion of the guest molecule in the β-CD cavity. This outcome was indeed evident when the complex formation between $1Cl_3$ and β-CD was monitored by ^{1}H NMR spectroscopic analysis in D_2O with varying concentrations of β-CD. Figure 5 reveals that on the addition of increasing amounts of β-CD, the resonance of the aromatic protons of $1Cl_3$ in the ^{1}H NMR spectrum were shifted upfield, whereas the signals for the aromatic protons of uncomplexed $1Cl_3$ remain unaffected. These signals indicate that the exchange between the free and bound guest with β-CD is slow on the ^{1}H NMR timescale. The upfield shifts seen in Figure 5 are most prominent ($\Delta\delta \approx 0.68$ ppm) for the three protons of the benzyl ring H_a, H_b, and H_c relative to the other two aromatic protons H_g and H_f ($\Delta\delta \approx 0.10$ and 0.07 ppm, respectively) of the phenyl ring of the TPA core in $1Cl_3$. This behavior suggests that the benzyl ring of $1Cl_3$ occupies a more shielded environment of the hydrophobic β-CD cavity in the inclusion complex. Figure 5 also reveals that on the formation of an inclusion complex with β-CD both H_d and H_e of $1Cl_3$ are shifted downfield.

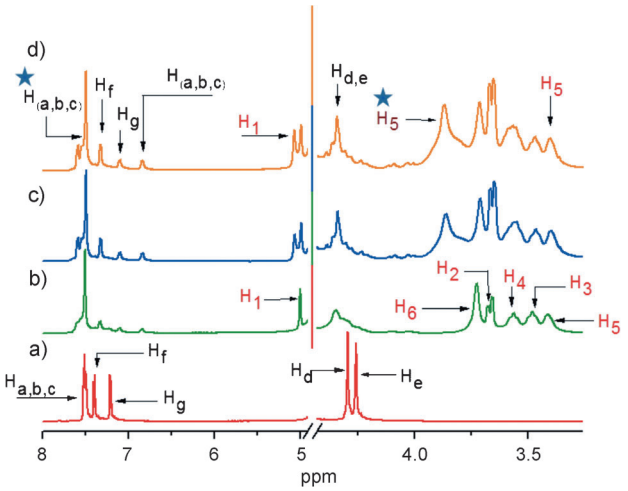

Figure 5. Partial ^{1}H NMR spectra (500 MHz, D_2O, 298 K) of a solution of $1Cl_3$ (8.4×10^{-3} M) with increasing [β-CD]. a) In the absence of β-CD and in the presence of b) 1.0, c) 2.0, and d) 3.0 equivalents of β-CD. The spectrum portrays a system of slow exchange, such that the two observable sets of signals that correspond to the complexed and uncomplexed (denoted by star) species.

These findings signify hydrogen-bond formation between these protons and the hydroxy functionality of the $-CH_2OH$ groups of the narrower rim of β-CD. A significant upfield shift for the protons of β-CD, positioned inside the cavity (i.e., H_3 and H_5) and the protons located near the narrow rim (i.e., H_6) of β-CD are also evident on inclusion-complex formation (Figure 5). The chemical shifts for the protons H_2 and H_4 positioned outside the cavity are insignificant on formation of the inclusion complex. All these data tend to confirm the formation of the "host–guest" inclusion complex $1Cl_3\cdot3\,$β-CD.

The information regarding the side of inclusion of the guest $1Cl_3$ into the β-CD cavity, that is, whether through the narrower or wider rim of β-CD, could be derived from the relative change in the chemical shift values for the H_3 and H_5 protons of the host molecule β-CD. It is reported that in general $\Delta\delta_{H_3} > \Delta\delta_{H_5}$ for the inclusion of the guest molecule through the wider rim side of β-CD and vice versa.[23] In the present study, the observed chemical shift of H_3 ($\Delta\delta_{H_3}=$ 0.50 ppm upfield shift) is more prominent than that for H_5 ($\Delta\delta_{H_5}=0.46$ ppm upfield shift), thus confirming the penetration of $1Cl_3$ through the wider rim side of β-CD (Figure 6). The 2D NOESY spectrum revealed cross-peaks between the aromatic protons and the H_5 and H_6 protons of β-CD (see the Supporting Information).

To study the involvement of the three binding sites of $1Cl_3$ with β-CD, ^{1}H NMR spectroscopic studies were performed with a series of solutions for which the initial concentration of $1Cl_3$ was kept constant at 8.4 mM, while the concentration of β-CD was systematically varied. On the

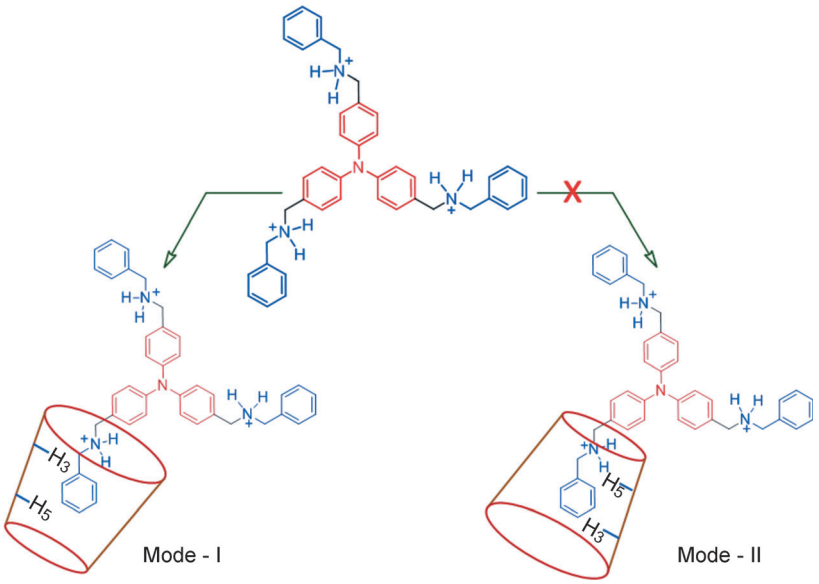

Figure 6. Schematic diagram to reveal the mode of penetration of $1Cl_3$ in the β-CD cavity on the inclusion-complex formation.

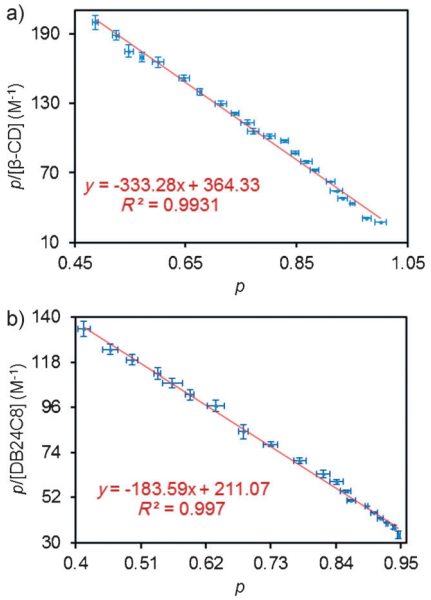

Figure 7. a) Scatchard plot for the complexation of $\mathbf{1}Cl_3$ with β-CD, where p is the fraction of $-NCH_2$ units of $\mathbf{1}Cl_3$ that exist as the included complex with β-CD as the host component (D_2O, 25 °C, $[\mathbf{1}Cl_3]_0 = 8.4 \times 10^{-3}$ M; error bars in $p = \pm 0.01$; error bar in $p/[\beta\text{-CD}] = \pm 2.88$). b) Complexation of $\mathbf{1}(PF_6^-)_3$ with DB24C8, where p is the fraction of $-NCH_2$ units of $\mathbf{1}(PF_6^-)_3$ bound as the included complex with DB24C8 as the host (CD_2Cl_2/CD_3CN (4:1, v/v), 25 °C, $[\mathbf{1}(PF_6^-)_3] = 7.6 \times 10^{-3}$ M; error bars in $p = \pm 0.01$; error bar in $p/[\text{DB24C8}] = \pm 2.37$).

basis of these data, the extent of complexation p was determined[22d] and a Scatchard plot[22] was constructed (Figure 7a). The linear nature of this plot demonstrates that the complex formation between $\mathbf{1}Cl_3$ and β-CD is statistical, that is, the three binding sites behave independently. The average association constant[22] $K_{av} = (3.4 \pm 12.8) \times 10^2\ M^{-1}$ was evaluated from the intercept and the slope of the plot.[24] As the complexation process was slow on the ^{1}H NMR timescale, the stoichiometry of the complex was determined by simple integration of the ^{1}H NMR signals for the relevant protons of the free and complexed $\mathbf{1}Cl_3$ and was found to be 1:3. ESI-MS measurements provided evidence for the 1:3 binding stoichiometry and the formation of the host–guest complex $\mathbf{1}Cl_3 \cdot 3\,\beta$-CD (Table 1).

Complexation of $\mathbf{1}(PF_6)_3$ with DB24C8: Formation of a host–guest complex between $\mathbf{1}(PF_6)_3$ and DB24C8 in a nonpolar solvent was established by ^{1}H NMR spectroscopic analysis. Earlier reports reveal that pseudorotaxanes exist in equilibrium with the individual components in a completely dissociated form.[25] Various nonbonding interactions present in the thus-formed pseudorotaxane are responsible for the stability of the included complex (i.e., the pseudorotaxane) over its precursors (i.e., the macrocyclic host and thread as the guest). In the present study, a slow kinetic exchange (on the ^{1}H NMR timescale at 500 MHz) as a result of the surmountable steric barrier for the slippage of the DB24C8 ring over the relatively bulky benzyl unit was present. This behavior accounts for observed signals in the ^{1}H NMR spectra for respective protons of $\mathbf{1}(PF_6)_3$ and DB24C8 that exist in the free and complexed forms (Figure 8). The signal for H_d and H_e of the uncomplexed benzyl moiety of $\mathbf{1}(PF_6)_3$ appear at 4.21 and 4.14 ppm, which were shifted downfield on the formation of an inclusion complex and appeared at 4.63 ppm. An increase in the intensity of this signal at 4.63 ppm was observed with an increase in the concentration of DB24C8. The percentage of ammonium ion-based thread $\mathbf{1}(PF_6)_3$ that was present as the complexed form was evaluated by comparison of the integration of these two sets of signals, which varied from 42.1 to 96.3% when [DB24C8] = 6.2–56.1 mM. A similar downfield shift was reported for the methylene protons in the ^{1}H NMR spectra of complexes formed between DB24C8 and substituted dibenzylammonium cations.[26] Interestingly, a gradual upfield shift for the signals for the H_d and H_e protons of uncomplexed $\mathbf{1}(PF_6)_3$ was also observed on an increase in the concentration of DB24C8 during the ^{1}H NMR spectroscopic titration process.

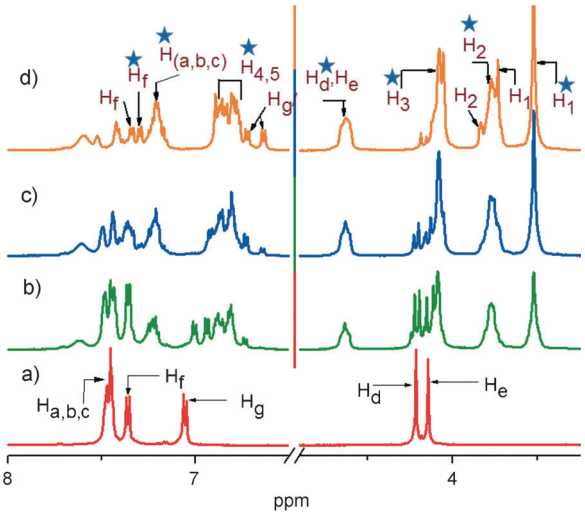

Figure 8. Partial ^{1}H NMR spectra (500 MHz, D_2O, 298 K) of $\mathbf{1}(PF_6)_3$ with varying [DB24C8] (CD_2Cl_2/CD_3CN (4:1, v/v), 25 °C, $[\mathbf{1}(PF_6^-)_3] = 7.6 \times 10^{-3}$ M). a) In the absence of DB24C8 and in the presence of b) 1.0, c) 2.0, and d) 3.0 equivalents of DB24C8. The spectrum portrays a system of slow exchange, such that the two observable sets of signal correspond to the complexed (denoted by star) and uncomplexed DB24C8.

The gradual upfield shift of the uncomplexed benzylic protons H_d and H_e with an increasing concentration of the crown ether as the host component has also been observed by many research groups. Gibson et al. concluded for analogous systems that the buildup of the concentration of PF_6^- ions around the free quaternary ammonium ion during the inclusion-complex formation was not responsible for this shift.[22d] Stoddart and co-workers reported that a similar upfield shift is the consequence of the shielding effect from a π-stacked catechol ring.[27] Figure 8 reveals that in the present study the ^{1}H NMR signals for the $-OCH_2$ groups of the crown ether moieties are shifted upfield on complexation, which is an observation that is consistent with the previous reports in which similar upfield shifts were registered for DB24C8 and its derivatives upon complexation with diben-

zylammonium ions.[28] Upfield shifts are evident for all the aromatic protons of **1**$(PF_6)_3$ with increasing concentration of DB24C8 (Figure 8). The aromatic protons of DB24C8 are also shifted upfield on complexation, which is used to estimate the extent of complexation.

To study the relationship between the three binding sites of **1**$(PF_6)_3$ during the complex-formation process with DB24C8, ^{1}H NMR spectroscopic studies were performed on a series of dichloromethane/acetonitrile (4:1 v/v) solutions, for which the initial concentration of **1**$(PF_6)_3$ was kept at 7.68 mM and the concentration of DB24C8 was varied systematically. The *p* value was evaluated for these data and a Scatchard plot[22] was prepared (Figure 7b). The linear nature of this plot demonstrated that the complexation between **1**$(PF_6)_3$ and DB24C8 was statistical. From the intercept and the slope of the plot, $K_{av}=(1.9\pm6.7)\times10^2\,M^{-1}$ was evaluated.[29] The value of the average binding constant, evaluated following the same method adopted by Gibson et al.,[22d] for the corresponding tritopic ammonium guest 1,3,5-tris[*para*-(benzylammoniomethyl)phenyl] benzene trishexafluorophosphate and DB24C8 was $K_{av}=1.5\times10^2\,M^{-1}$ in CD_3CN. The lower polarity of the solvent medium ($CD_2Cl_2/CD_3CN=4:1$, v/v) in the present study could have contributed to a slightly higher value for K_{av} than that reported in CD_3CN.[22d] As the complexation process is slow on the ^{1}H NMR timescale, the stoichiometry of the complex was determined to be 1:3 by simple integration of the signals for the relevant protons in the free and complexed states. A binding stoichiometry of 1:3 was also confirmed from mass-spectrometric analysis (ESI-MS and MALDI-TOF; Table 1).

UV/Vis, fluorescence, and TCSPC studies: The UV/Vis and steady-state emission spectra for **1**X_3 ($X=Cl^-$, PF_6^-) were recorded in either water or dichloromethane (the relevant data are summarized in Table 2). The absorption spectrum of **1**Cl_3 in water showed an intense absorption band ($\varepsilon=2.8\times10^4\,L\,mol^{-1}\,cm^{-1}$) with an absorption maxima at $\lambda_{max}=309$ nm; whereas, $\lambda_{max}=317$ nm and $\varepsilon=3.7\times10^4\,L\,mol^{-1}\,cm^{-1}$ in dichloromethane. The observed absorption band was attributed to the triphenylamine-based π–π* transition. Absorption spectra for **1**Cl_3 were also recorded in water in the presence of three equivalents of CB[7] or β-CD. Interestingly, the addition of CB[7] induced a hyperchromism (ca. 7%) of the absorption band for **1**Cl_3, whereas a hypochromism of (ca. 6%) was observed when β-CD was used. No shift in the absorption maxima was observed in either case (see the Supporting Information). However, both features are indicative of binding of the dye to the macrocycle. The absorption spectrum of **1**$(PF_6)_3$ was recorded in presence of three equivalents of DB24C8 in dichloromethane, thus giving two maxima at $\lambda=281$ and 317 nm. The band at $\lambda=281$ nm was assigned for a DB24C8-based transition, which for free DB24C8 appeared at $\lambda=274$ nm. The band at $\lambda=317$ nm showed hypochromism (ca. 6%) when recorded in the presence of DB24C8, though no shift in the absorption maxima at $\lambda=317$ nm was observed.

The solvatochromic behavior of **1**X_3 was examined in different solvents with varying polarities (see the Supporting Information). A redshift of $\Delta\lambda=20$ nm in the emission band maxima was observed in cyclohexane ($\lambda_{max,\,em}=364$ nm for $\lambda_{ext}=309$ nm) and water ($\lambda_{max,\,em}=384$ nm for $\lambda_{ext}=309$ nm). In contrast, no shift in the absorption band was noticed with the change in media polarity. Interestingly, the emission spectra were broader with a solvent of higher polarity. The observed redshift and broader emission band could be attributed to an internal charge-transfer excited state, which is also very likely to be twisted in geometry due to the flexible nature of the molecule. Such behavior is not uncommon for numerous fluorescent molecules with donor–acceptor components, including TPA derivatives.[30]

These results also support the nonvanishing dipole moment of TPA in solution and are consistent with a molecular geometry that is slight nonplanar at the central nitrogen atom. The solvatochromic behavior was also supported by a decrease in the fluorescence quantum yield with an increase in solvent polarity ($\Phi=0.0099$ and 0.0119 in water and CH_2Cl_2, respectively). The lower quantum yield in water is presumably due to the lowered energy of the increased stabilization of the highly polar intramolecular charge-transfer (ICT) states.[31] The emission band maxima for **1**Cl_3 in water appeared at $\lambda_{max}=388$ nm for excitation at $\lambda=309$ nm and a significant change in the luminescence intensity was observed in the presence of CB[7] and β-CD (Figure 9). In the case of CB[7], an enhancement of 430% was observed ($\Phi=0.0283$) for the highest concentration of CB[7] used (CB[7]/**1**$Cl_3=8:1$; $[\mathbf{1}Cl_3]=9.2\times10^{-6}$ M; Figure 9a).

However, the changes were different for β-CD from that observed for CB[7] (Figure 9b): an increase of 260% in luminescence intensity ($\Phi=0.0182$) and a blueshift of $\Delta\lambda=15$ nm for the band maxima were observed at the highest concentration of β-CD used (i.e., β-CD/**1**$Cl_3=15:1$). Molecule **1**Cl_3 showed weak emission in the free state, and the respective quantum yield was $\Phi=0.0099$. This difference in fluorescent enhancement of **1**Cl_3 in the presence of CB[7] and β-CD is essentially due to the

Table 2. Spectral parameters for **1**X_3.

Host–guest system	ε [$L\,mol^{-1}\,cm^{-1}$]	λ_{abs} [nm]	λ_{em} [nm]	Φ
1Cl_3	2.8×10^{4}[a]	309[a]	388[a]	0.0099[a]
1$(PF_6)_3$	3.7×10^{4}[b]	317[b]	369,[b] 482,[b] 370[c]	0.0119[b] 0.0580[c]
1Cl_3·3 CB[7]	2.9×10^{4}[a]	309[a]	384[a]	0.0283[a]
1Cl_3·3 β-CD	2.6×10^{4}[a]	307[a]	380[a]	0.0182[a]
1$(PF_6)_3$ ·3 DB24C8	3.5×10^{4}[b]	317[b]	368,[b] 500[b]	0.0386[b]

[a] Measurements were performed in water. [b] Measurements were performed in dichloromethane. [c] Measurements were performed in glycerol.

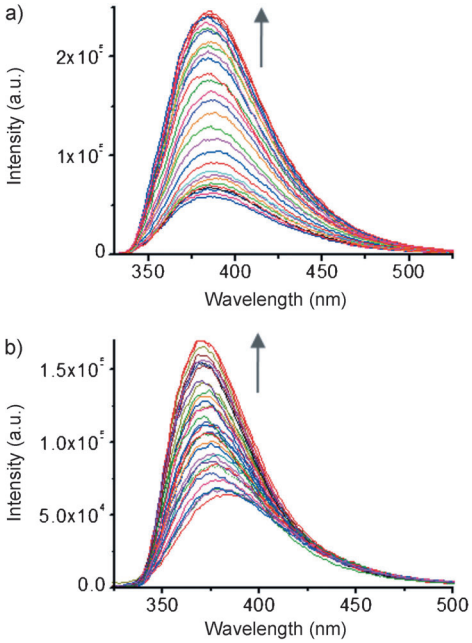

Figure 9. Fluorescence spectra of $\mathbf{1}Cl_3$ in water upon the addition of increasing concentrations of a) CB[7] and b) β-CD ($\mathbf{1}Cl_3 = 9.2\times10^{-6}$ M, $\lambda_{exc} = 309$ nm).

fundamental differences in the topology of the upper and lower rims of the two classes of macrocyclic host and the difference in their binding abilities. To develop a better understanding about the origin of this effect, additional measurements were made in glycerol, a medium known for its high viscosity so that restricted molecular movements could be induced. The quantum yield recorded for $\mathbf{1}X_3$ in glycerol was $\Phi = 0.058$, which is significantly higher than those determined in the presence of the macrocyclic hosts CB[7] and β-CD (Table 2). This outcome suggests that the origin of this binding-induced fluorescence enhancement is attributed mainly to the restricted internal rotation of the molecule on the formation of the inclusion complex. It is widely accepted that internal rotation generally provides additional channels for nonradiative de-excitation of the excited states.[32] Additionally, recent reports also revealed significant fluorescence enhancements for TPA-based dye molecules as a result of restricted rotational freedom upon binding to DNA and RNA matrices.[33] In the present study, an appreciable steric hindrance was induced in $\mathbf{1}Cl_3$ to inhibit the rotational freedom of the TPA-based core on the formation of inclusion complexes with these macrocyclic hosts. Additionally, the reduction of local polarity experienced by the TPA derivative within the macrocyclic host cavity, relative to that in aqueous solution, might have also contributed to the observed fluorescence enhancement.

Luminescence-decay profiles for the excited state were measured for $\mathbf{1}Cl_3$ in the presence and absence of CB[7] and β-CD by using time-correlated single-photon counting with a nano-sized light-emitting diode (nano-LED) as an excitation source at $\lambda = 280$ nm. Luminescence decay, monitored at $\lambda = 388$ nm for $\mathbf{1}Cl_3$, showed an average lifetime of 0.80 ns. The decay profiles were also recorded in the presence of three molar equivalents of CB[7] and β-CD (Table 3) to give average lifetimes of 1.05 and 1.45 ns, respectively. The increase in the average lifetime of $\mathbf{1}Cl_3$ in the presence of CB[7] and β-CD also supports the restriction of internal rotation in the excited state on inclusion-complex formation. This behavior along with the decrease in the local polarity is expected to decrease the deactivation processes through a nonradiative pathway and to subsequently enhance the luminescence quantum yield.

Table 3. Fluorescence lifetime τ data obtained by using a nano-LED as an excitation source ($\lambda = 280$ nm) and monitoring the wavelength λ_{em} in water and dichloromethane at 25 °C.

Host–guest system	λ_{em} [nm]	τ [ns]	χ^2
$\mathbf{1}Cl_3$	388[a]	0.80	0.91
$\mathbf{1}Cl_3\cdot3$ CB[7]	388[a]	1.05	0.92
$\mathbf{1}Cl_3\cdot3$ β-CD	388[a]	1.45	1.06
DB24C8	300[b]	0.57	1.12
$\mathbf{1}[PF_6]_3$	380[b]	2.98	1.17
$\mathbf{1}(PF_6)_3\cdot3$ DB24C8	300[b]	0.42 (61.3 %), 2.23 (38.7 %)	0.91

[a] Measurements were performed in water. [b] Measurements were performed in dichloromethane. χ^2 is a numerical value that reflects the overall goodness of fit.

The electronic spectra for $\mathbf{1}(PF_6)_3$ and its inclusion complex with DB24C8 in dichloromethane were different from those for $\mathbf{1}Cl_3\cdot3$ CB[7] and $\mathbf{1}Cl_3\cdot3$ β-CD (see the inset of Figure 10a and the Supporting Information). For the 1:3 complex between DB24C8 with $\mathbf{1}(PF_6)_3$ (i.e., $\mathbf{1}(PF_6)_3\cdot3$ DB24C8), the absorption spectrum of the [4]pseudorotaxane complex was different from its individual components $\mathbf{1}(PF_6)_3$ and DB24C8. The redshifted absorption band for the [4]pseudorotaxane complex appeared at $\lambda = 282$ nm relative to the absorption band maxima for DB24C8 at $\lambda = 275$ nm. This noticeable shift in the absorption band maxima is indicative of an interaction in the ground state for the [4]pseudorotaxane.

Changes in the luminescence spectrum for $\mathbf{1}(PF_6)_3$ recorded in the absence and presence of three molar equivalents of DB24C8 were even more significant. DB24C8 in dichloromethane showed an emission band with maxima at $\lambda_{max} = 310$ nm on excitation at $\lambda = 280$ nm (where DB24C8 absorbs predominantly); however, the emission intensity at $\lambda = 310$ nm for [4]pseudorotaxane was completely quenched when compared with free DB24C8. Subsequently, an increase in emission intensity at $\lambda = 369$ nm, which corresponds to a $\mathbf{1}(PF_6)_3$-based emission, was observed when compared with that for a comparable concentration of free $\mathbf{1}(PF_6)_3$. These steady-state emission results suggest a possible energy-transfer (ET) process that involves the low-lying excited state of DB24C8 as the donor state and the even lower excited state of $\mathbf{1}(PF_6)_3$ as the acceptor state. To check the thermodynamic feasibility of such an ET process, it is essential to have some idea about the relative energies for the LUMO for the chromophores, namely, DB24C8 and $\mathbf{1}(PF_6)_3$,

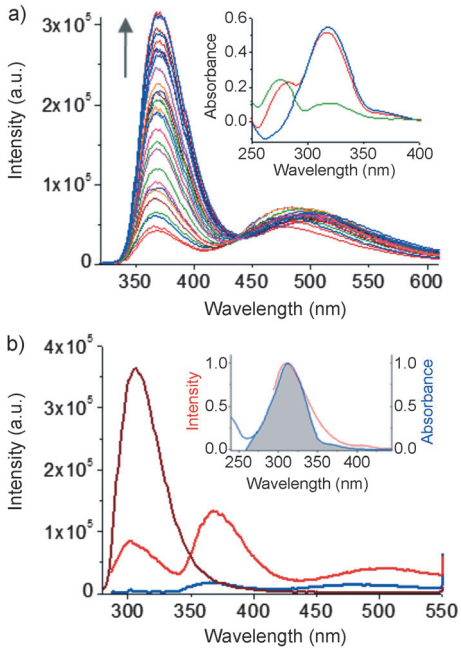

Figure 10. a) Fluorescence spectra of $\mathbf{1}(PF_6)_3$ in dichloromethane with increasing [DB24C8] ($\lambda_{exc}=310$ nm, $[\mathbf{1}(PF_6)_3]=7.3\times10^{-6}$ M; inset: absorption spectra for $\mathbf{1}(PF_6)_3$ (blue line) DB24C8 (green line), and $\mathbf{1}(PF_6)_3\cdot3$DB24C8 (red line)). b) Emission spectra for DB24C8 at $\lambda_{exc}=280$ nm (purple line = DB24C8 (2.2×10^{-5} M), red line = 3.0 equiv DB24C8 + $\mathbf{1}(PF_6)_3$, blue line = $\mathbf{1}(PF_6)_3$ (7.3×10^{-6} M); inset: emission and absorption spectral overlap for DB24C8 and $\mathbf{1}(PF_6)_3$, respectively).

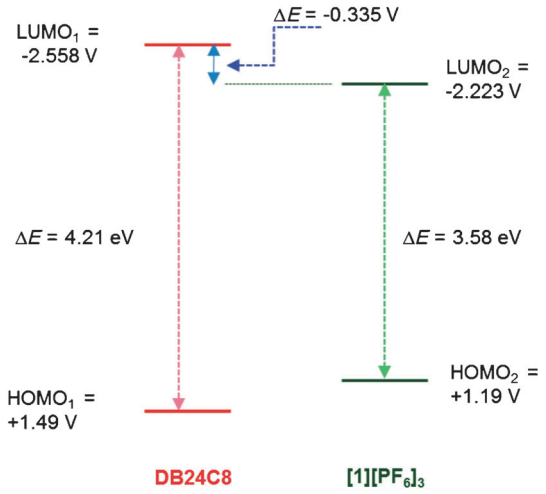

Figure 11. Relative energies for the HOMO and LUMO levels for DB24C8 and $\mathbf{1}(PF_6)_3$, which were evaluated from the respective ground-state redox potentials and $E_{0\text{-}0}$ values.

in the [4]pseudorotaxane complex. Cyclic voltammetry (CV) experiments were carried out in dichloromethane/acetonitrile and revealed two oxidation processes: the first at $E=+1.49$ V (versus Ag/AgCl; corresponds to $HOMO_1$) for the DB24C8-based redox process and the second at $E=+1.19$ V (versus Ag/AgCl; corresponds to $HOMO_2$) for the $\mathbf{1}(PF_6)_3$-based redox process. Furthermore, the LUMO energy levels for the respective components were calculated by using the value of the optical-band gap ($E_{0\text{-}0}$) obtained from the intersecting wavelength of the normalized emission and excitation spectra, which were $E=4.21$ and 3.58 eV for DB24C8 and $\mathbf{1}(PF_6)_3$, respectively.

These values enabled us to evaluate the energies for the LUMO for these two chromophores, which were $E=-2.72$ and -2.39 V for $LUMO_1$ for DB24C8 and $LUMO_2$ for $\mathbf{1}(PF_6)_3$, respectively (Figure 11). Thus, the energy gap (i.e., $LUMO_1-LUMO_2$) of $\Delta E=-0.33$ V supports the thermodynamic feasibility of an ET process. More importantly, a closer look at the emission spectra for $\mathbf{1}(PF_6)_3$ and the absorption spectra for DB24C8 reveals a significant spectral overlap (see the inset of Figure 10a), thus further corroborating the possibility of the Förster resonance energy-transfer (FRET) mechanism. Additionally, the normalized absorption spectrum for the [4]pseudorotaxane complex was identical with the normalized excitation spectrum for $\mathbf{1}(PF_6)_3$ ($\lambda_{ems}=369$ nm), thus further confirming an efficient ET process.[34]

To quantify the ET efficiency, we compared the fluorescence quantum yields of the donor in the presence and absence of the acceptor using Equation (1), in which Φ_{donor} and $\Phi_{donor-acceptor}$ correspond to the fluorescence quantum efficiency of the donor in the absence and presence of the acceptor, respectively.

$$\Phi_{ET}=1-\frac{\phi_{donor-acceptor}}{\phi_{donor}} \quad (1)$$

The ET quantum yield for $\mathbf{1}(PF_6)_3\cdot3$DB24C8 complex was calculated to be 71.2%. The ET rate was evaluated by using Equation (2) and was found to be $4.3\times10^9\ s^{-1}$. These data enable us to calculate the Förster distance of $R_0=43.1$ Å by using a standard equation reported previously [Eq. (2)].[35]

$$K_{ET}=\frac{1}{\tau_{donor}}\left(\frac{1}{(1/\Phi_{ET})-1}\right) \quad (2)$$

To obtain more information about such ET processes, fluorescence lifetime measurements were carried out for $\mathbf{1}(PF_6)_3\cdot3$DB24C8, DB24C8, and $\mathbf{1}(PF_6)_3$ in dichloromethane with a nano-LED as an excitation source at $\lambda=280$ nm. The decay profile of DB24C8 was best fit to a single-exponential process with $\tau=0.57$ ns for $\lambda_{mon}=300$ nm. However, a similar study for a 1:3 mixture of $\mathbf{1}(PF_6)_3$ and DB24C8 ($\lambda_{mon}=300$ nm) revealed that the lifetime of the DB24C8-based decay component decreased from 0.57 to 0.41 ns, thus suggesting an efficiency of only 28% for the ET process [see Eq. (1) and Table 3].

The apparent disagreement in the ET efficiency, calculated on the basis of the quantum yields (71.2%) and time-resolved spectra (28%) suggests the possibility of other quenching mechanisms being operational in addition to the resonance ET process. The results of the ^1H NMR spectroscopic studies described earlier suggest incomplete complex

formation between DB24C8 and $\mathbf{1}(PF_6)_3$ for the [4]pseudorotaxane formation. Presumably there is a spectral overlap of the emission of the uncomplexed DB24C8 with the absorption spectra of $\mathbf{1}(PF_6)_3$, and the light emitted by DB24C8 is in turn absorbed by $\mathbf{1}(PF_6)_3$, thus causing the trivial sensitization effect between the free components in addition to the FRET. Therefore, quenching of the DB24C8 emission due to this trivial sensitization effect might have added up to overall quenching of the donor chromophore (i.e., DB24C8), which in turn showed the greater quenching and thus the higher ET efficiency. The absence of any rise-time when the fluorescence decay was monitored at the acceptor emission suggests a very fast ET, which could not be identified by the resolution of our spectrophotometer.[36]

Conclusion

In summary, the complexation behavior of a newly synthesized TPA derivative with three different host molecules, namely, β-CD, CB[7], and DB24C8, has been demonstrated. MALDI-TOF mass-spectrometric and ^{1}H NMR and 2D NOESY spectroscopic experiments revealed a 1:3 binding stoichiometry, the extent of complexation, and the topology of the inclusion processes. ^{1}H NMR spectroscopic studies also revealed a cooperative binding process for CB[7], whereas statistical binding prevailed for hosts β-CD and DB24C8. Enhanced fluorescence and an increase in the average lifetime of $\mathbf{1}X_3$ on inclusion-complex formation with β-CD or CB[7] can be attributed to the restricted internal rotation of the TPA core. This finding was confirmed by steady-state and time-resolved emission studies. The choice of DB24C8 as a host component offered us the unique opportunity to study the binding-induced FRET process that involves DB24C8 as a donor molecule and $\mathbf{1}(PF_6)_3$ as an acceptor. This outcome was established by using ground-state redox-potential and steady-state luminescence data. A trivial ET and a FRET process are proposed to be the reason for the quenching of the DB24C8-based luminescence for studies with $\mathbf{1}(PF_6)_3$ and DB24C8. Thus, the present studies have revealed that fluorescence spectroscopy can also be used as a tool to probe the structural confinement imposed on TPA derivatives by macrocyclic hosts in addition to detailed NMR spectroscopic studies. More importantly, the results of the steady-state and time-resolved fluorescence studies also helped to understand the change in environment of the TPA core from the bulk of the solvent medium to a hydrophobic environment during complexation with β-CD and CB[7].

Experimental Section

General: Tris(*para*-formylphenyl)amine and benzylamine were obtained from Sigma–Aldrich and were used as received without any further purification. NH_4PF_6 was recrystallized from ethanol before use. All the solvents were of reagent grade and were procured from S.D. Fine Chemicals (India). All the solvents were dried and distilled prior to use following standard procedures.

The ^{1}H NMR spectra were recorded on a Bruker 500 MHz FT NMR Advance-DPX 500 spectrometer at room temperature (25 °C). The chemical shifts δ are reported in parts per million (ppm) and relative to trimethylsilane (TMS) as an internal standard. The coupling constants J are given in Hertz. ESI mass-spectrometric measurements were carried out on a Waters Q-TOF Micro instrument. The UV/Vis spectra were obtained by using a Cary 500 Scan UV/Vis–NIR spectrometer. Steady-state emission spectra at room temperature were obtained on a Fluorolog (Horiba Jovin Yvon) luminescence spectrofluorimeter. Time-resolved emission studies were carried out using the TCSPC technique (Edinburgh Instruments F900). The redox values were measured by cyclic volotametry (CV) with a bipotentiostat (AFCBPI, PINE Instrument Co). A conventional three-electrode cell assembly was used with a platinum-disk electrode as the working electrode, a platinum wire as a counterelectrode, and an Ag/AgCl electrode as a reference electrode. All the measurements were carried out in dichloromethane/acetonitrile containing 0.1 M tetrabutylammonium hexafluoroborate $[(n\text{-}C_4H_9)_4NBF_4]$ as a supporting electrolyte. The scan rate used was 0.5 V s^{-1}, ferrocene (Fc) was used as an internal standard for the CV studies, and the Fc/Fc^+ couple appeared at $E=$ 0.395 V. The methodologies adopted for the calculation of errors in solution preparation and instrumental analysis are provided in the Supporting Information.

Synthetic procedure of $\mathbf{1X_3}$: Benzylamine (0.5 g, 5.2 mmol) was added to tris(*para*-formylphenyl)amine (0.5 g, 1.5 mmol) dissolved in dry acetonitrile/methanol (30 mL, 1:1, v/v), and the reaction mixture was stirred vigorously at room temperature. After 24 h, methanol (20 mL) was added to the reaction mixture, which was cooled to 0 °C. $NaBH_4$ (0.5 g) was added portionwise to the stirred cooled reaction mixture, which was stirred for another 1 h at 0 °C. The reaction mixture was allowed to reach the room temperature and stirred for a further 2 h. The solvent was removed under reduced pressure, the residue was extracted three times with $CHCl_3$ and water, and the organic layers were combined and dried over anhydrous sodium sulfate. The solvent was removed under reduced pressure to give the crude product, which was purified on a silica gel with $CH_3OH/CHCl_3$ (4:96, v/v) as the eluent. The desired compound was isolated as a sticky brown solid. A solution of HCl (concentrated HCl (0.5 mL) dissolved in acetone (2 mL)) was added dropwise to the sticky solid dissolved in acetone (20 mL) and stirred for 2 h. A brown solid was formed, which was isolated by filtration and air dried (0.6 g, 65 %). Salt $\mathbf{1}(PF_6)_3$ was isolated as a precipitate by adding an aqueous solution of NH_4PF_6 to a solution of $\mathbf{1}Cl_3$ in acetone, collected by filtration, and dried over P_2O_5. M.p. $\mathbf{1}(PF_6)_3$: 92 °C, $\mathbf{1}Cl_3$: 190 °C; ^{1}H NMR (500 MHz, CD_2Cl_2, 298 K): $\delta=$ 7.47–7.45 (15 H, m), 7.37 (6 H, d, $J=$ 8.5 Hz), 7.06 (6 H, d, $J=$ 8.5 Hz), 4.21 (6 H, s), 4.14 ppm (6 H, s); ^{13}C NMR (500 MHz, CD_3CN, 298 K): $\delta=$ 147.6, 131.2, 129.7, 129.2, 128.6, 124.9, 123.8, 116.9, 50.6 ppm; HRMS (ESI): m/z calcd for $[C_{42}H_{46}N_4]^{4+}$: 606.3722; found: 606.3697 (error = ±4.2 ppm).

Acknowledgements

A.D. thanks DST (India) and CSIR (India) for supporting this research. A.K.M., M.S., and P.D. acknowledge CSIR for their research fellowships. The authors are thankful to Prof. H.W. Gibson of Virginia Polytechnic Institute and University (USA) for his suggestion and help in the interpretation of certain parts of the NMR data and error analysis. We also thank Dr. S. Basa of CSMCRI for his help in evaluating cumulative errors. The authors are thankful to the reviewers for their suggestions, which were very helpful in improving this manuscript.

[1] a) G. Schill, *Catenanes, Rotaxanes, and Knots*, Academic Press, New York, **1971**. pp. 1–270; b) J. L. Atwood, J. E. D. Davies, D. D. MacNicol, F. Vogtle, *Comprehensive Supramolecular Chemistry*, Pergamon, Oxford, **1996**, pp. 1–970; c) H.-J. Schneider, A. Yatsimirsky,

Principles and Methods in Supramolecular Chemistry,Wiley, Chichester, **2000**, pp. 137–190; d) F. Huang, H. W. Gibson, *Progr. Polym. Sci.* **2005**, *30*, 982–1018; e) Z. Niu, H. W. Gibson, *Chem. Rev.* **2009**, *109*, 6024–6046; f) G. Wenz, *Adv. Polym. Sci.* **2009**, *222*, 1–54; g) A. Harada, A. Hashidzume, H. Yamaguchi, Y. Takashima, *Chem. Rev.* **2009**, *109*, 5974–6023; h) E. Coronado, P. Gavina, S. Tatay, *Chem. Soc. Rev.* **2009**, *38*, 1674–1689; i) P. Gavina, S. Tatay, *Curr. Org. Synth.* **2010**, *7*, 24–43; j) L. Fang, M. A. Olson, D. Benitez, E. Tkatchouk, W. A. Goddard, J. F. Stoddart, *Chem. Soc. Rev.* **2010**, *39*, 17–29; k) D. Thibeault, J.-F. Morin, *Molecules* **2010**, *15*, 3709–3730.

[2] a) Z. Chen, A. Lohr, C. R. Saha-Moeller, F. Wuerthner, *Chem. Soc. Rev.* **2009**, *38*, 564–5840.

[3] a) G. A. Jeffrey, *An Introduction to Hydrogen Bonding*, Oxford University Press, New York, **1997**, pp. 1–303; b) T. Takata, N. Kihara, *Rev. Heteroatom. Chem.* **2000**, *22*, 197–218; c) J.-M. Zhao, Q.-S. Zong, T. Han, J. F. Xiang, C.-F. Chen, *J. Org. Chem.* **2008**, *73*, 6800–6806; d) J.-B. Guo, Y. Jiang, C.-F. Chen, *Org. Lett.* **2010**, *12*, 5764–5767; e) J.-B. Guo, J. F. Xiang, C.-F. Chen, *Eur. J. Org. Chem.* **2010**, 5056–5062.

[4] a) A. G. Street, S. L. Mayo, *Proc. Natl. Acad. Sci. USA* **1999**, *96*, 9074–9076; b) A. C. Bhasikuttan, J. Mohanty, W. M. Nau, H. Pal, *Angew. Chem.* **2007**, *119*, 4198–4200; *Angew. Chem. Int. Ed.* **2007**, *46*, 4120–4122.

[5] a) M. Suresh, A. K. Mandal, M. K. Kesharwani, N. N. Adarsh, B. Ganguly, R. K. Kanaparthi, A. Samanta, A. Das, *J. Org. Chem.* **2011**, *76*, 138–144; b) A. K. Mandal, M. Suresh, A. Das, *Org. Biomol. Chem.* **2011**, *9*, 4811–4817.

[6] a) W. L. Yu, J. Pei, W. Huang, A. J. Heeger, *Chem. Commun.* **2000**, 681–682; b) D. Troadec, G. Veriot, A. Moliton, *Synth. Met.* **2002**, *127*, 165–168; c) J. P. Chen, H. Tanabe, X. C. Li, T. Thoms, Y. Okamura, K. Ueno, *Synth. Met.* **2003**, *132*, 173–176.

[7] a) Y. Yasuda, T. Kamiyama, Y. Shirota, *Electrochim. Acta* **2000**, *45*, 1537–1541; b) J. Ostrauskaite, H. R. Karickal, A. Leopold, D. Haarer, M. Thelakkat, *J. Mater. Chem.* **2002**, *12*, 3469.

[8] B. P. Chandra, *Indian J. Pure Appl. Phys.* **1980**, *18*, 743–746.

[9] a) H. B. Lueck, J. L. McHale, W. D. Edwards, *J. Am. Chem. Soc.* **1992**, *114*, 2342–2348; b) G. Meijer, G. Berden, W. L. Meerts, H. E. Hunziker, M. S. de Vries, H. R. Wendt, *Chem. Phys.* **1992**, *163*, 209–222.

[10] a) M. Malagoli, J. L. Bredas, *Chem. Phys. Lett.* **2000**, *327*, 13–17; b) I. Reva, L. Lapinski, N. Chattopadhyay, R. Fausto, *Phys. Chem. Chem. Phys.* **2003**, *5*, 3844–3850.

[11] a) P. Wei, X. D. Bi, Z. Wu Z. Xu, *Org. Lett.* **2005**, *7*, 3199–3202; b) Z. Fang, T. L. Teo, L. Cai, Y. H. Lai, A. Samoc, M. Samoc, *Org. Lett.* **2009**, *11*, 1–4.

[12] a) D. Hellwinkel, M. Melan, *Chem. Ber.* **1971**, *104*, 1001–1016; b) D. Hellwinkel, G. Aulmich, M. Melan, *Chem. Ber.* **1974**, *107*, 616–627; c) D. Hellwinkel, W. Schmidt, *Chem. Ber.* **1980**, *113*, 358–384.

[13] a) A. L. Koner, W. M. Nau, *Supramol. Chem.* **2007**, *19*, 55–66.

[14] a) K. Kim, *Chem. Soc. Rev.* **2002**, *31*, 96–107; b) J. W. Lee, S. Samal, N. Selvapalam, H.-J. Kim, K. Kim, *Acc. Chem. Res.* **2003**, *36*, 621–630; c) J. Lagona, C. Mukhopadhyay, L. Isaacs, *Angew. Chem.* **2005**, *117*, 4922–4949; *Angew. Chem. Int. Ed.* **2005**, *44*, 4844–4870.

[15] a) W. Ong, A. E. Kaifer, *J. Org. Chem.* **2004**, *69*, 1383–1385; b) A. D. St-Jacques, I. W. Wyman, D. H. Macartney, *Chem. Commun.* **2008**, 4936–4938; c) N. Noujeim, L. Leclercq, A. R. Schmitzer, *J. Org. Chem.* **2008**, *73*, 3784–3790; d) I. W. Wyman, D. H. Macartney, *J. Org. Chem.* **2009**, *74*, 8031–8038; e) N. Noujeim, B. jouvelet, A. R. Schmitzer, *J. Phys. Chem. B* **2009**, *113*, 16159–16168; f) Y. Zeng, Y. Li, M. Li, G. Yang, Y. Li, *J. Am. Chem. Soc.* **2009**, *131*, 9100–9106; g) I. W. Wyman, D. H. Macartney, *Org. Biomol. Chem.* **2010**, *8*, 253–260; h) M. Florea, W. M. Nau, *Angew. Chem. Int. Ed.* **2011**, *50*, 9338–9342.

[16] a) D. M. Rudkevich, *Angew. Chem.* **2004**, *116*, 568–581; *Angew. Chem. Int. Ed.* **2004**, *43*, 558–571; b) N. Saleh, A. L. Koner, W. M. Nau, *Angew. Chem.* **2008**, *120*, 5478; *Angew. Chem. Int. Ed.* **2008**, *47*, 5398–5401; c) I. W. Wyman, D. H. Macartney, *Org. Biomol. Chem.* **2008**, *6*, 1796–1801; d) R. Wang, D. Bardelang, M. Waite, K. A. Udachin, D. M. Leek, K. Yu, C. I. Ratcliffe, J. A. Ripmeester, *Org. Biomol. Chem.* **2009**, *7*, 2435–2439; e) C. Li, J. Li, X. Jia, *Org. Biomol. Chem.* **2009**, *7*, 2699–2703.

[17] a) B. D. Wagner, N. Stojanovic, A. I. Day, R. J. Blanch, *J. Phys. Chem. B* **2003**, *107*, 10741–10746; b) J.-X. Liu, L.-S. Long, R.-B. Huan, L.-S. Zheng, *Inorg. Chem.* **2007**, *46*, 10168–10173.

[18] a) *Chem. Rev.* **1998**, *98*, 1741–2076 (a special issue on cyclodextrins); b) A. C. Bhasikuttan, H. Pal, J. Mohanty, *Chem. Commun.* **2011**, *47*, 9959–9971.

[19] a) N. Yamaguchi, L. M. Hamilton, H. W. Gibson, *Angew. Chem.* **1998**, *110*, 3463–3466; *Angew. Chem. Int. Ed.* **1998**, *37*, 3275–3279; b) S. J. Cantrill, A. R. Pease, J. F. Stoddart, *J. Chem. Soc. Dalton Trans.* **2000**, 3715–3734, and references therein; c) S. Liu, C. Ruspic, P, Mukhopadhya, S. Chakrabarty, P. Y. Javaliz, L. Isaacs, *J. Am. Chem. Soc.* **2005**, *127*, 15959–15967; d) P. Mukhopadhyay, P. Y. Javaliz, L. Isaacs, *J. Am. Chem. Soc.* **2006**, *128*, 14093–14102; e) H. G. Gibson, J. W. Jones, L. N. Zakharov, A. L. Rheingold, C. Slebodnick, *Chem. Eur. J.* **2011**, *17*, 3192–3206.

[20] a) T. B. Stolwijk, E. J. R. Sudhölter, D. N. Reinhoudt, S. Harkema, *J. Org. Chem.* **1989**, *54*, 1001.

[21] a) V. Sindelar, K. Moon, A. E. Kaifer, *Org. Lett.* **2004**, *6*, 2665–2668.

[22] a) A. G. Marshall, *Biophysical Chemistry*, Wiley, New York, **1978**; pp. 70–77; b) B. Perlmutter-Hayman, *Acc. Chem. Res.* **1986**, *19*, 90–96; c) K. A. Connors, *Binding Constants*, Wiley, New York, **1987**, pp. 78–86; d) H. W. Gibson, N. Yamaguchi, L. Hamilton, J. W. Jones, *J. Am. Chem. Soc.* **2002**, *124*, 4653–4665; e) F. Huang, J. W. Jones, H. W. Gibson, *J. Org. Chem.* **2007**, *72*, 6573–6576.

[23] a) T. Nakajima, M. Sunagawa, T. hirohashi, K. Fujioka, *Chem. Pharm. Bull.* **1984**, *32*, 383–400; b) D. Salvatierra, C. Jaime, A. Virgili, F. S. Ferraando, *J. Org. Chem.* **1996**, *61*, 9578–9581; c) M. S. Ali, F. J. Asmat, *Incl. Phenom. Macroc. Chem.* **2007**, *59*, 191–196.

[24] Scatchard plot analysis (Figure 7a) reveals $K_{av}=3.4\times10^2\,M^{-1}$ ($K_{av}=(-\text{slope}+\text{intercept})/2$); $K_{av}=4.33K_3$, $K_2=3K_3$, and $K_1=9K_3$; for a statistical binding of 1:3, the ratio of the binding constants is $K_1/K_2/K_3=9:3:1$;[22d] $K_1=7.2\times10^2$, $K_2=2.4\times10^2$, and $K_3=0.8\times10^2\,M^{-1}$.

[25] a) P. R. Ashton, I. Baxter, M. C. T. Fyfe, F. M. Raymo, N. Spencer, J. F. Stoddart, A. J. P. White, D. J. Williams, *J. Am. Chem. Soc.* **1998**, *120*, 2297–2307.

[26] a) P. R. Ashton, P. J. Campbell, E. J. T. Chrystal, P. T. Glink, S. Menzer, D. Philp, N. Spencer, J. F. Stoddart, P. A. Tasker, D. J. Williams, *Angew. Chem.* **1995**, *107*, 2001–2004; *Angew. Chem. Int. Ed. Engl.* **1995**, *34*, 1869–1871; b) P. R. Ashton, R. Ballardini, V. Balzani, M. Gómez-López, S. E. Lawrence, M.-V. Martínez-Díaz, M. Montalti, A. Piersanti, L. Prodi, J. F. Stoddart, D. J. Williams, *J. Am. Chem. Soc.* **1997**, *119*, 10641–10651; c) T. Han, C. F. Chen, *Org. Lett.* **2006**, *8*, 1069–1072.

[27] T. Chang, A. M. Heiss, S. J. Cantrill, M. C. T. Fyfe, A. R. Pease, S. J. Rowan, J. F. Stoddart, D. J. Williams, *Org. Lett.* **2000**, *2*, 2943–2946.

[28] a) P. R. Ashton, P. J. Campbell, E. J. T. Chrystal, P. T. Glink, S. Menzer, D. Philp, N. Spencer, J. F. Stoddart, P. A. Tasker, D. J. Williams, *Angew. Chem.* **1995**, *107*, 1997–2001; *Angew. Chem. Int. Ed. Engl.* **1995**, *34*, 1865–1869; b) A. M. Elizarov, S. H. Chiu, P. T. Glink, J. F. Stoddart, *Org. Lett.* **2002**, *4*, 679–682.

[29] Scatchard plot analysis (Figure 7b) reveals $K_{av}=1.9\times10^2\,M^{-1}$ ($K_{av}=(-\text{slope}+\text{intercept})/2$); $K_{av}=4.33K_3$, $K_2=3K_3$, and $K_1=9K_3$; for a statistical binding of 1:3, the ratio of the binding constants is $K_1/K_2/K_3=9:3:1$;[22d] $K_1=4.1\times10^2$, $K_2=1.3\times10^2$, and $K_3=0.4\times10^2\,M^{-1}$.

[30] a) Z. Diwu, C. Zhang, R. P. Klaubert, J. Haughland, *J. Photochem. Photobiol. A* **2000**, *131*, 95–100; b) H. Detert, V. Schmidt, *J. Phys. Org. Chem.* **2004**, *17*, 1051–1056; c) R. Lartia, C. Allain, G. Bordeau, F. Schmidt, C. F. Debuisschert, F. Charra, M. P. T. Fichou, *J. Org. Chem.* **2008**, *73*, 1732–1744.

[31] a) C. Le Droumaguet, O. Mongin, M. H. V. Werts, M. Blanchard-Desce, *Chem. Commun.* **2005**, 2802–2804; b) H. Y. Woo, B. Liu, B. Kohler, D. Korystov, A. Mikhailovsky, G. C. Bazan, *J. Am. Chem. Soc.* **2005**, *127*, 14721–14729.

[32] G. Oster, Y. Nishijima, *J. Am. Chem. Soc.* **1956**, *78*, 1581–1584.

[33] C. Allain, F. Schmidt, R. Lartia, G. Bordeau, C. F. Debuisschert, F. Charra, P. Tauc, M. P. Teulade-Fichou, *ChemBioChem* **2007**, *8*, 424–433.

[34] B. Valeur, *Molecular Fluorescence Principles and Application*, Wiley-VCH, **2001**, pp. 110–113.
[35] H. M. Watrob, C. P. Pan, M. D. Barkley, *J. Am. Chem. Soc.* **2003**, *125*, 7336–7343.
[36] a) J. Y. Wang, J. M. Han, J. Yan, Y. Ma, J. Pei, *Chem. Eur. J.* **2009**, *15*, 3585–3594; b) M. Y. Berezin, S. Achilefu, *Chem. Rev.* **2010**, *110*, 2641–2684.

Received: October 1, 2011
Published online: February 17, 2012

